# DESALINATION OF BRACKISH WATER WITH THERMALLY REGENERABLE ION-EXCHANGE RESIN USING A SOLAR POND

**A. A. Kerestecioglu and A. M. El-Nashar***

*Department of Mechanical Engineering, Florida Institute of Technology, Melbourne, Florida 32901, U.S.A.*

الخلاصــة :

أجريت عدة تجارب عملية لتحديد أنسب قيم لعوامل التشغيل في مبدل أيوني يمكن أعادة شحنه بواسطة الطاقة الحرارية وقد أستخدمت في هذه التجارب مادة أمبرلايت أكس دي ٥ المنتجة بواسطة شركة روم وهاس الأمريكية . وقد أستخدمت نتائج هذه التجارب العملية في تعميم محطة لتحلية المياه الجوفية ذات سعة تتراوح بين ٣٠٠٠ إلى ١٠٠٠٠ متر مكعب يومياً وتستخدم هذا النوع من المبدل الأيوني . ويعاد شحن أعمدة التبادل الأيوني في هذه المحطة بواسطة الطاقة الحرارية المنتجة بواسطة برك شمسية . وقد تم في هذه الدراسة عمل نموذج حسابي لتحديد أنسب تصميم لمثل هذه المحطة وأستخدم النموذج مع الحاسب الإلكتروني لتحديد أقل تكاليف للمحطة .

## ABSTRACT

Several laboratory scale experiments were conducted in order to find the optimum operating conditions of a thermally regenerable resin. The resin used was Amberlite XD-5 manufactured by Rohm and Haas Co. Using the experimental results for the resin performance, detailed design and optimization were done for a brackish water desalination plant having a capacity ranging from 3000 to 10 000 $m^3$/day. A salt-gradient solar pond is used to supply the thermal energy for resin regeneration. A computer model was developed to optimize the plant design and minimize capital cost.

*Present address: *Water and Electricity Department, P.O. Box 219, Abu Dhabi, U.A.E.*

0377-9211/83/03209-12$1.20

# DESALINATION OF BRACKISH WATER WITH THERMALLY REGENERABLE ION-EXCHANGE RESIN USING A SOLAR POND

## NOTATION

| | |
|---|---|
| $A$ | Heat transfer area, $m^2$ |
| $A_r$ | Cross-sectional area of IX columns, $m^2$ |
| $C_f$ | Salt concentration of feed, ppm TDS |
| $C_{min}$ | Minimum thermal capacity, kJ/sK |
| $C_{max}$ | Maximum thermal capacity, kJ/sK |
| $C_m$ | Defined as (no. of tubes/no. of tube rows)$^{1/2}$ in heat exchanger |
| $C_{hx}$ | Capital cost of heat exchanger, \$ |
| $C_p$ | Capital cost of pump, \$ |
| $C_i$ | Capital cost of each plant component, \$ |
| $C$ | Total capital cost of plant, \$ |
| $D$ | Depth of solar pond, m |
| $D_1$ | Heat exchanger tube inside diameter |
| $D_p$ | Resin particle diameter, m |
| $f$ | Adjustment factor for solar insolation |
| $f_1$ | Friction factor inside heat exchanger tubes |
| $f_2$ | Friction factor on shell side of heat exchanger |
| $f_m$ | Friction factor for flow through resin bed |
| $F$ | Pump discharge, l/min |
| $g$ | Gravitational acceleration, $m/s^2$ |
| $G_1$ | Tube side mass velocity, $kg/m^2s$ |
| $G_2$ | Shell side mass velocity, $kg/m^2s$ |
| $G$ | Fluid superficial mass velocity in resin bed, $kg/m^2s$ |
| $I_p$ | Annual average useful insolation, $kW/m^2$ |
| $I_h$ | Annual average insolation on horizontal surface, $kW/m^2$ |
| $L$ | Ion-exchange column length, m |
| $L$ | Annual average thermal load on solar pond, kW |

## 1. INTRODUCTION

Desalination of brackish water can be achieved by several methods. These can generally be classified into two groups. Methods in the first group physically separate water from the brine solution; these include the reverse osmosis, distillation, and freezing processes. The second group is composed of processes that separate salt from the brine solution, such as the electrodialysis and ion-exchange processes.

The ion-exchange process, which belongs to the second group, has not been used widely for desalination of brackish water for the main reason that for every equivalent of salt removed from the solution, at least one equivalent of regenerant must be used, and most likely discarded to the environment [1]. Therefore, in recent years, attention has been directed to thermally regenerated ion-exchange resins and regenerant recycle systems [1, 2, 3].

The possibility of using a solar pond to provide the thermal energy required by a desalination plant utilizing the thermally regenerated ion-exchange resin seems to offer certain advantages for desalting brackish water. These advantages are:

(a) no chemicals are needed for regeneration;
(b) process requires no phase change (as in distillation) and therefore no special materials for construction;
(c) no high pressures (as in reverse osmosis) are required;
(d) no electric current is needed to effect salt separation (as in electrodialysis).

The main disadvantage of the ion-exchange process seems to be its limitation for the desalting of brackish water with low salinity. For a single stage the maximum feed salinity is 3000 ppm total dissolved solids.

The main objective of this work is to study the technical feasibility and optimization of a solar desalination plant which uses a thermally regenerated ion-exchange (IX) resin in combination with a solar pond. The study is divided into two main parts:

(a) an experimental investigation of the performance of the IX resin to be used, namely Amberlite XD-5 provided by Rohm and Haas Co.; and
(b) the design and optimization of a desalination plant using the experiental data obtained and the prediction of capital cost estimates.

## 2. THE CYCLING ZONE ADSORPTION PROCESS

The process which uses the thermally regenerated ion-exchange resin to desalt brackish water is called Cycling Zone Adsorption (CZA), which was developed by Shih and Pigford [12]. The process operates on the principle of cyclic adsorption and desorption of one or more solutes using the resin as a solid adsorbent. This results in an alternating solute-depleted and solute-enriched effluent. Such a process has important advantages. It requires no chemical regeneration and can use low grade thermal energy such as could be obtained from solar ponds.

The operation of the CZA process can be described with reference to Figure 1. The brackish feed solution is passed through a fixed bed of solid particles. The fluid and solid system can be transferred from one equilibrium state to another by a shift in its temperature. The system fluctuates between cold $T_c$ and hot $T_h$.

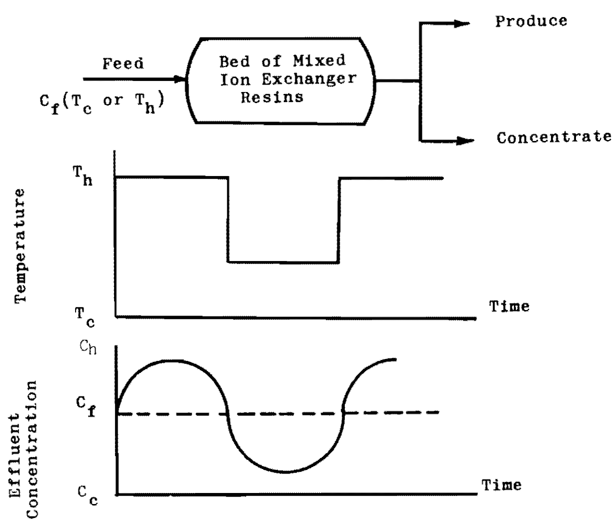


*Figure 1. Cycling Zone Adsorptive Process*

Let the system be initially in equilibrium at $T_c$. The solid particles are saturated with the solutes in the feed and the effluent concentration is the same as that of the feed. If the system temperature is raised to $T_h$, solutes that were previously held on the solid will be expelled into the fluid. The bed effluent will then have a concentration higher than that of the feed until the system reaches its new equilibrium state. However, just before the feed concentration begins to increase, if the bed temperature is decreased to $T_c$, the solid takes up solutes from the fluid and temporarily holds it on the solid. During this period, the effluent will be solute-depleted. Switching again to the high temperature will result in solute-enriched effluent.

The result is a cyclically repeating wave of fluid concentration in the effluent, part of the wave is at a concentration above the feed concentration $C_f$ and part at a concentration below it. Each part is collected separately.

The equilibrium between a mixed bed of resins and a aqueous solution of sodium chloride can be expressed by the following equation:

$$\overline{RCOOH} + \overline{R_3N} + Na^+ + Cl^-$$
$$\rightleftharpoons \overline{RCOO^- \, Na^+} + \overline{R_3 \, NH^+Cl^-}$$

The salt is adsorbed by the resin as a result of transfer of hydrogen ions from the acid to the base resin. This equilibrium is temperature dependent. There is a reduction in the number of exchange sites on both the acidic and basic resins upon heating and salt is therefore released in the solution. Salt is adsorbed onto the resin upon cooling.

## 3. EXPERIMENTAL

### 3.1. Test Apparatus

The thermally regenerable ion-exchange resin used in the experimental program was Amberlite XD-5 manufactured by Rohm and Haas Co. Since little information was supplied by the manufacturer on the performance of this resin, it was necessary to conduct an experimental program to obtain the necessary data.

A simple bench scale thermally cycled ion-exchange apparatus was designed and built to evaluate the different process variables. The experimental set-up is shown in Figure 2. It consists of an insulated ion-exchange (IX) column, two constant temperature

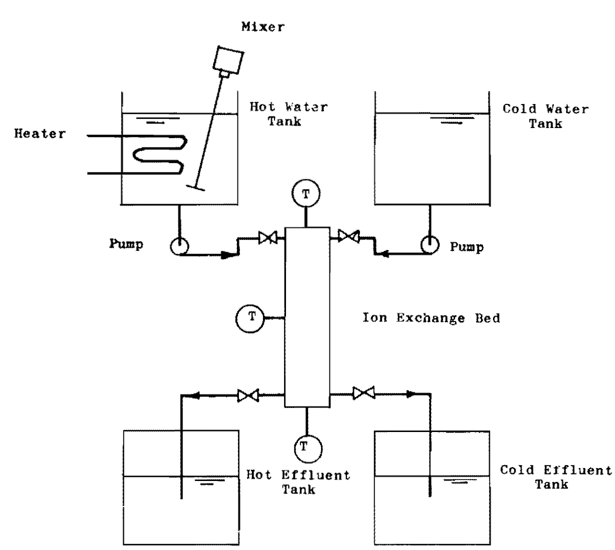


*Figure 2. Experimental Apparatus*

baths, and the necessary pipings and valves. A thermostatically controlled heater is inserted in the hot regenerant bath which is thermally insulated to minimize heat loss to the environment. The other tank contained cold saline feed water. The IX column which contained the resin was instrumented by three copper-constant thermocouples attached to the top, middle, and bottom of the column to monitor the fluid temperature.

To start the experiment a sodium chloride solution of known concentration was prepared and introduced into the two baths. The electric heater in the regenerant bath was turned on and the selected regeneration temperature was dialed on the heater thermostat. During the desalination period cold saline feed water was admitted into the IX column and the effluent was collected in a graduated tube.

The total dissolved solids (TDS) of the effluent in the graduated tube, which is a mixture average, was monitored continuously. The flow rate of the effluent from the column was also measured by timing a measured volume of water. The desalination period ended when the TDS of the mixture reached 500 ppm. At this time, the resin was assumed to be saturated and ready for regeneration.

In the regeneration period, hot regenerant fluid passes through the resin which causes the adsorbed salt to be desorbed in the regenerant fluid. During this period, the TDS of the effluent drops from a high initial value toward an equilibrium value equal to the TDS of the influent. At this point the regeneration period ends and the resin is ready for the next cycle.

Tests were conducted for different flow rates, salinities, temperatures, and column lengths in order to find the effect of these independent variables on the resin performance, namely the desalination and regeneration periods.

The resin received from Rohm and Haas was a composite acidic and basic mixture. The characteristics of this composite resin used in this study are shown below:

| | |
|---|---|
| Physical form | spherical particles |
| Resin density (dry) | 0.64 $gm/cm^3$ dry resin |
| Resin density (wet) | 0.43 $gm/cm^3$ wet resin |
| Void fraction (dry) | 0.42 dry resin |
| Void fraction (wet) | 0.45 wet resin |
| Bed expansion | 19.5% |

### 3.2. Experimental Results

Table 1 shows the results which were obtained during one typical complete cycle made up of a desalination and a regeneration period. More experimental results are given in [8]. These results give the column effluent concentration in ppm at different times during the desalination and regeneration period. For this particular cycle the feed (and regenerant) salt concentration was 1500 ppm and the mean regenerant temperature was 87°C.

**Table 1. Typical Experimental Data**

| Time (min) | Effluent concentration (ppm) | |
|---|---|---|
| 0.0 | 590 | |
| 3.0 | 422 | |
| 6.0 | 436 | Desalination period |
| 9.0 | 518 | |
| 12.0 | 562 | |
| 15.0 | 4180 | |
| 18.0 | 3216 | |
| 21.0 | 2496 | Regeneration period |
| 24.0 | 1982 | |
| 27.0 | 1500 | |

$q_h = 5.4\ cm^3/min\ cm^2$
$q_c = 7.0\ cm^3/min\ cm^2$
$T_m = 87°C$
$C_f = 1500$ ppm (feed and regenerant concentration)

At the beginning of the desalination period, the salt concentration of the column effluent was 590 ppm and this dropped to 422 ppm after 3 minutes of operation. During the remaining part of the desalination period, the effluent salinity continued to increase until the time when the accumulated effluent salinity reached 500 ppm where the desalination period ended and the regeneration period began.

The effluent concentration reached its maximum value at the start of the regeneration period. Throughout the regeneration period, the concentration dropped until finally it reached that of the regenerant concentration (same as feed concentration) and at this point the regeneration period ended.

The resin salt capacity (eq/l) depends on the feed (or loading) and regenerant temperatures, feed (and regenerant) salt concentration, and the pH. Typical results are shown in Figure 3 for a feed and regenerant concentration of 500 ppm NaCl, for two regeneration temperature of 80°C and 95°C, and for a pH of 5.73. As expected, the resin salt capacity increases with an increase in the regeneration temperature and a reduction in the feed (loading) temperature.

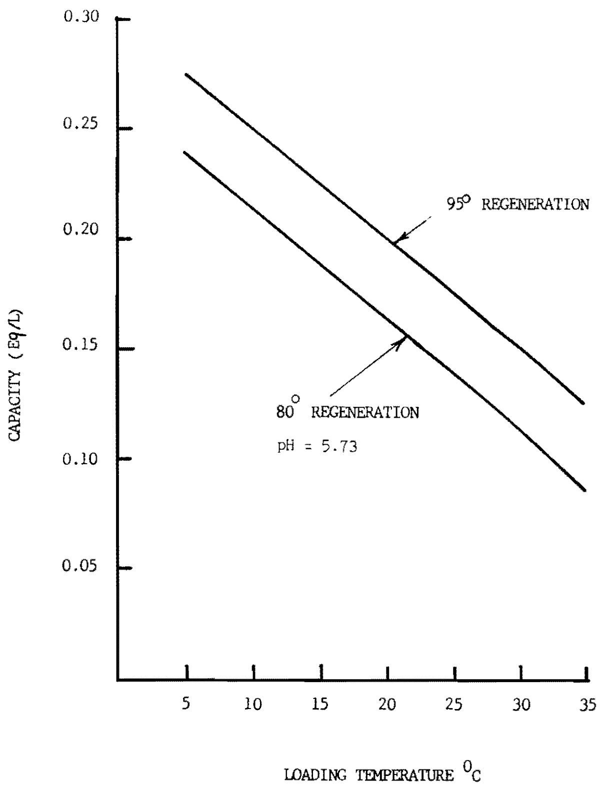


*Figure 3. Effect of Loading and Regeneration Temperature on Capacity of Amberlite XD-5 at 500 ppm NaCl*

## 4. PLANT DESCRIPTION

A schematic of the solar desalination plant is shown in Figure 4. The main components are the ion-exchange columns which contain the thermally regenerable resin, the solar pond for providing the thermal energy for regenerating the resin, the main heat exchanger for heating the feed water to the required regeneration temperature and the preheater to raise the feed water temperature before entering the main heat exchanger. The plant consists also of a number of control valves to regulate the flow of hot and cold fluids and pumps to generate the necessary flow rates. Five valves are shown in Figure 4, V1, V2, V3, V4, and V5.

During the desalination period, valves V1 and V4 will be open and valves V2, V3, and V5 will be closed. During this period pretreated brackish feed water will pass through the IX columns and its salinity will be reduced to potable water level. At the end of this period, the IX resin will become saturated and will need regeneration.

At the end of the desalination period, valves V1 and V4 will be closed and V2, V3, and V5 will be opened to start the regeneration period. During this period the IX resin will be regenerated by passing hot brackish water through the columns. During the regeneration period the feed water will be heated first by passing through the preheater then by flowing through the main heat exchanger. The preheater is designed to take advantage of the hot regenerating fluid discharged from the IX columns during the regeneration period. This will result in reducing the thermal load on the solar pond therefore reducing its size.

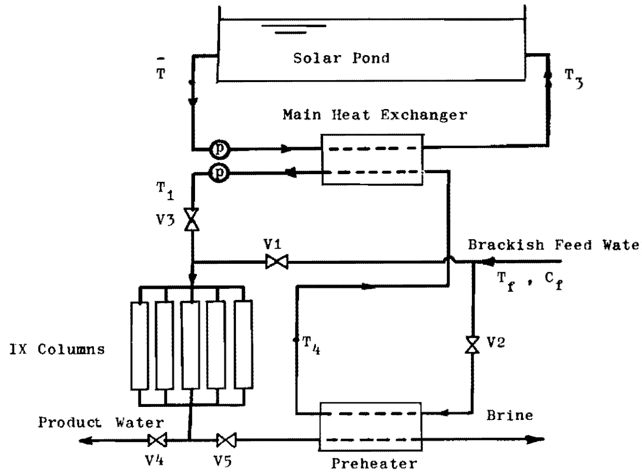


*Figure 4. Schematic of the Solar Desalination Plant*

In the main heat exchanger, the feed water will be heated to the regeneration temperature by the solar pond fluid located in the storage layer. The pond is of the general salt-gradient type as suggested by Tabor [13] and Weinberger [14]. Temperature inversions take place in these ponds with higher temperatures in the bottom layers than near the surface.

## 5. OPTIMIZATION OF THE DESALINATION PLANT

### 5.1. Mathematical Modeling of the Plant Components

*(a) Ion-Exchange Resin Columns*

The mathematical model used for the IX columns was based on the experimental data obtained using Amberlite XD-5 resin. In order to represent the data in a mathematical form, a multiple regression analysis was carried out using the SPSS [4] computer program available at the computer center at Florida Institute of Technology.

The independent variables used in the regression analysis program were the desalination and regeneration flow rates per unit column cross-sectional area ($q_c$ and $q_h$), the column length ($L$), the mean regeneration temperature ($T_m$), and the salinity of the feed water ($C_f$) expressed in ppm, TDS. The dependent variables were the desalination and regeneration times $t_d$ and $t_r$. The desalination time is the time required for the accumulated product to reach a salinity of 500 ppm. The regeneration time is defined as the time required by the effluent regenerating fluid to reach a salinity equal to that of the influent. The following expressions were found to fit the experimental data very closely.

(i) *Desalination Period*

$$t_d = -2.021\, q_c - 0.7185\times10^{-3}\, C_f + 26.69,$$
$$\text{for } L = 15\text{ cm},\ 500\text{ ppm} \le C_f \le 2500\text{ ppm},$$
$$3.0\text{ cm}^3/\text{min cm}^2 \le q_c \le 7.0\text{ cm}^2/\text{min cm}^2. \quad (1)$$

$$t_d = -2.174\, q_c + 0.433L + 22.531,$$
$$\text{for } 10\text{ cm} \le L \le 30\text{ cm},\ C_f = 2500\text{ ppm},$$
$$3.0\text{ cm}^3/\text{min cm}^2 \le q_c \le 7.0\text{ cm}^3/\text{min cm}^2. \quad (2)$$

(ii) *Regeneration Period*

$$t_r = -1.0704\, q_h + 0.194 T_m + 0.146\times10^{-2} C_f - 2.744,$$
$$\text{for } L = 15\text{ cm},\ 500\text{ ppm} \le C_f \le 2500\text{ ppm},$$
$$3.0\text{ cm}^3/\text{min cm}^2 \le q_h \le 8.0\text{ cm}^3/\text{min cm}^2$$
$$70^\circ\text{C} \le T_m \le 90^\circ\text{C}. \quad (3)$$

$$t_r = 0.2904L - 0.849 q_h + 0.0692 T_m - 1.208,$$
$$\text{for } 10\text{ cm} \le L \le 30\text{ cm},\ C_f = 2500\text{ ppm},$$
$$3.0\text{ cm}^3/\text{min cm}^2 \le q_h \le 8.0\text{ cm}^3/\text{min cm}^2,$$
$$70^\circ\text{C} \le T_m \le 90^\circ\text{C}. \quad (4)$$

The temperature $T_m$ is the mean regeneration temperature defined as:

$$T_m = \frac{T_1 + T_2}{2}. \quad (5)$$

(b) *Salt-Gradient Solar Pond*

The required solar pond surface area is a function of the annual average pond temperature, annual average ambient temperature, annual average solar insolation, the annual thermal load, and the latitude. The calculation procedure suggested in [6] is used. Assuming a circular pond, the radius can be expressed by:

$$R = \frac{U_e\Delta T + \{(U_e\Delta T)^2 + \bar{L}[\bar{I}_p - (U_s + U_b)\Delta T]/\pi\}^{0.5}}{\bar{I}_p - (U_s + U_b)\Delta T}. \quad (6)$$

In Equation (6) $U_e$, $U_s$, and $U_b$ are the average heat loss coefficients from the edges, the surface, and the bottom, respectively. $\Delta T$ is the difference between the annual average pond temperature $\bar{T}$ and the annual average ambient temperature:

$$\Delta T = \bar{T} - \bar{T}_a.$$

$\bar{I}_p$ is the annual average useful insolation which can be expressed as [6, 7]:

$$\bar{I}_p = \bar{I}_h f \overline{\tau\alpha}, \quad (7)$$

where $\bar{I}_h$ is the annual average isolation on a horizontal surface, f is an adjustment factor [6], and $\overline{\tau\alpha}$ is an average transmissivity absorptivity product for the pond fluid.

The solar pond depth $D$ can be calculated indirectly from the following equation:

$$\bar{T} = T_{min} = \frac{[(a + dD)^2 + (b + CD)^2]^{0.5}}{5.2327D^2 + 7.5445(U_s + U_b)^2}, \quad (8)$$

where $T_{min}$ is the minimum desired pond temperature, and $a$, $b$, $c$, and $d$ are functions of the ambient temperature, solar insolation, average and maximum loads, and are described in detail in [8]. A solution for the depth $D$ requires an iterative approach which can best be handled on a digital computer.

(c) *Main Heat Exchanger and Preheater*

For the analysis of the heat exchanger, the effectiveness–NTU method is used [9]. The effectiveness is defined as follows:

$$\varepsilon = \frac{C_h(T_{h1} - T_{h2})}{C_{min}(T_{h1} - T_{c1})}. \quad (9)$$

Since $C_h(T_{h1} - T_{h1}) = C_c(T_{c2} - T_{c1})$,

$$\varepsilon = \frac{C_c(T_{c2} - T_{c1})}{C_{min}(T_{h1} - T_{c1})}, \quad (10)$$

where the subscripts h1 and h2 on the temperature represent the inlet and exit of the hot stream and c1 and c2 represent the inlet and exit of the cold stream. $C_c$ and $C_{min}$ are the thermal capacity of the cold fluid and the minimum thermal capacity respectively.

Using counter flow heat exchangers, the effectiveness can be expressed in terms of the number of transfer units NTU and thermal capacities $C_{min}$ and $C_{max}$ [9]:

$$\varepsilon = \frac{1 - \exp\{-\text{NTU}[1 - (C_{min}/C_{max})]\}}{1 - (C_{min}/C_{max})\exp\{-\text{NTU}[1 - (C_{min}/C_{max})]\}}, \quad (11)$$

where $\text{NTU} = UA/C_{min}$, with $U$ as the overall heat transfer coefficient and $A$ the heat exchanger area.

For the pressure drop calculations, the tube side and the shell side are considered separately. For the tube side the pressure $P_1$ can be expressed as:

$$\Delta P_1 = \frac{f_1 G_1^2 L_1 N_1}{2 D_1 \rho_g}, \tag{12}$$

where $f_1$ is the friction factor, $G_1$ is the tube side mass velocity (mass flow rate per unit area), $L_1$ is the bundle length, $N_1$ is the number of tube side passes, and $D_1$ is the inside diameter of the tube. For the shell side the pressure drop $\Delta P_2$ can be calculated from the equation:

$$\Delta P_2 = \frac{f_2 G_2^2 n^{0.5} N_2}{2 \rho_g C_m}, \tag{13}$$

where $f_2$ is the friction factor, $G_2$ is the shell side mass velocity, $n$ is the number of tubes. $N_2$ is the number of passes across the tube bundle, and $C_m$ is as defined in the notation. Reference [10] should be consulted for detailed heat exchanger design.

### 5.2. Optimization of IX Column Operation

For continuous plant operation, the number of cycles per day, $n_c$ can be calculated from:

$$n_c = \frac{24 \times 60}{t_c + t_h}, \tag{14}$$

where $t_c$ and $t_h$ are expressed in minutes.

The daily hot water required for regeneration is

$$Q_h = q_h t_h n_c A_r, \tag{15}$$

where $A_r$ is the cross-sectional area of all the IX columns. Similarly, the daily amount of cold water feed that can be desalted can be calculated from:

$$Q_c = q_c t_c n_c A_r. \tag{16}$$

The objective here is to maximize $Q_c$ and to minimize the thermal energy required for regeneration, i.e. minimize $Q_h T_1$. The optimization program was developed using the Rosenbrock constrained method to obtain the optimum IX column operating conditions. This program is described and listed in [8].

### 5.3. General and Unit Cost Assumptions

The following general assumptions are made for the purpose of plant design and optimization:

(1) The plant will work continuously 24 hours per day.
(2) The plant capacity varies from 3000 to 10 000 m$^2$/day.
(3) The feed water is brackish water having a salt concentration ranging from 1000 to 2500 ppm TDS.
(4) The product water concentration is 500 ppm.
(5) The plant location is Miami, Florida.
(6) A source for pumping power is assumed available on the plant site.

The cost figures for the solar pond used in this study are given in Table 2.

**Table 2. Cost Figures for the Solar Pond**

| Component | Estimated cost |
|---|---|
| Earth moving | \$ 1.50/m$^3$ |
| Walls | \$40.00/m$^2$ installed |
| Liner | \$ 8.00/m$^2$ installed |
| Surface grid | \$ 1.50/m$^2$ installed |
| Salt | \$30.00/ton |

The cost data for the heat exchangers obtained from [10, 11] were updated using the ENR cost index. The updated data were fitted to a quadratic equation using the least squares technique. The resulting cost equation becomes:

$$C_{hx} = 621.45 + 23.86A + 0.156A^2, \tag{17}$$

where $C_{hx}$ is the heat exchanger installed cost and $A$ is the heat transfer area.

The cost of the Amberlite XD-5 resin was taken as \$19.30 per kg based on the manufacturers suggestions. The resin is not commercially available in large quantities at the present time, and therefore this cost figure may be subject to variations when the resin is introduced on the market.

The pump cost equation of [11] was also updated using the ENR cost index and is given below

$$C_p = 5.0778\left(\frac{F}{3.785}\right)0.585(14.7P)^{0.245}(14.7\Delta P)^{0.61}, \tag{18}$$

where $F$ is the pump discharge in liters per minute, $P$ is the suction pressure in atmospheres, and $\Delta P$ is the pump head in atmospheres. Capital cost estimates for other plant components like piping, valves, etc. are to be found in [8].

### 5.4. Plant Optimization

The criteria used for plant optimization is the minimization of the capital cost. Therefore, the objective function used can be written as follows:

$$C = \sum_{i=1}^{n} C_i,$$

where $C$ is the capital cost of the desalination plant and $C_i$ is the capital cost of each component, e.g. solar pond, IX columns, etc. The objective function given above was minimized subject to the following constraints:

$$70°C \leq \bar{T} \leq 90°C$$
$$70°C \leq T_1 \leq 87°C$$
$$\bar{T} - T_3 \leq 10°C$$
$$30°C \leq T_f \leq 21°C$$
$$1000 \text{ ppm} \leq C_f \leq 2500 \text{ ppm}$$
$$D \leq 6 \text{ m}.$$

The optimization procedure used is shown in Figure 5. Using the experimental data for the IX resin (Amberlite XD-5), the optimum resin operating conditions were found as described earlier. This will result in obtaining the optimum flow rates and desalination and regeneration periods as well as the regeneration temperature. Assuming a preheater exit temperature $T_4$ (see Figure 4), pond minimum temperature $T_{min}$ and pond average temperature $\bar{T}$, the pond area can be calculated using Equation (6). For an assumed value of pond depth, the value of $(\bar{T}\text{-}T_{min})$ is calculated from Equation (8) and compared with the assumed value. The depth is then decremented or incremented until the calculated $\Delta T$ agree with the assumed value.

Following the pond area and depth calculations, the heat transfer and pressure drop estimates are made for the preheater and main heat exchanger. The pump sizing are made after estimates of the pressure drop and flow rates through the loops are made. After each plant component sizing is conducted, the capital cost calculations are made. The cost figure is compared with that of the previous iteration and each of the variables $T_4$, $\Delta T$, and $\bar{T}$ are consequently changed by a finite value until the minimum cost is obtained.

A computer program was developed to carry out the above calculations using Fortran IV and was run on the VAX-11/70 computer at Florida Institute. A listing of this program is given in [8].

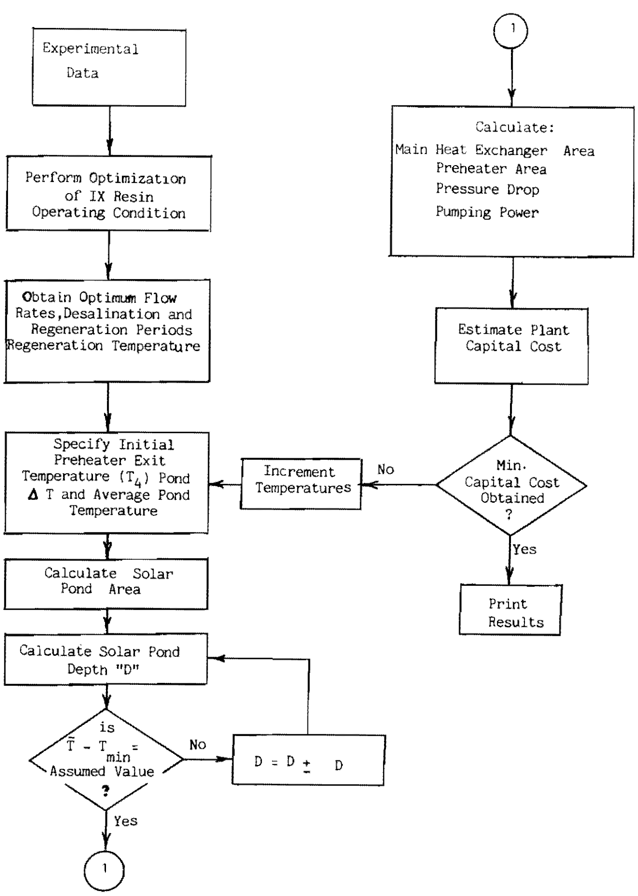


*Figure 5. Procedure for the Optimization Calculations*

## 6. RESULTS

The results of the optimization routine discussed above will be presented in this section. The optimization of the whole plant was divided into two parts: first the operating conditions of the IX columns was optimized using the experimental data and a computer algorithm [8] and then the whole desalination plant was optimized using the results of the first optimizing program.

It should be pointed out that the results obtained are for the city of Miami, Florida and such results will naturally be location dependent. The cost estimates obtained are based on the economic ground rules presented in Section 5.3.

### 6.1. Effect of Feed Water Temperature

The effect of the feed water temperature on the main heat exchanger area requirement is shown in Figure 6. Since the feed water has to be heated to 80°C to regenerate the IX resin, a higher feed water temperature would result in a reduction of the main heat exchanger load and a corresponding reduction in its heat exchanger area.

A high feed water temperature would also result in a smaller solar pond radius and fluid withdrawal rate (see Figures 7 and 8) which is a direct consequence of a small thermal load on the solar pond.

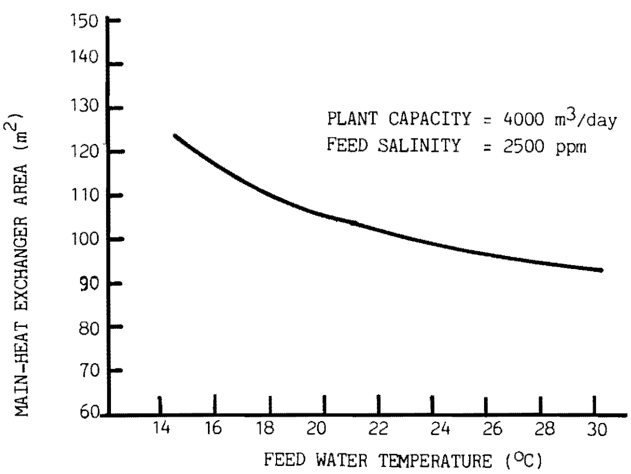


*Figure 6. Effect of Feed Water Temperature on Main Heat Exchanger Area*

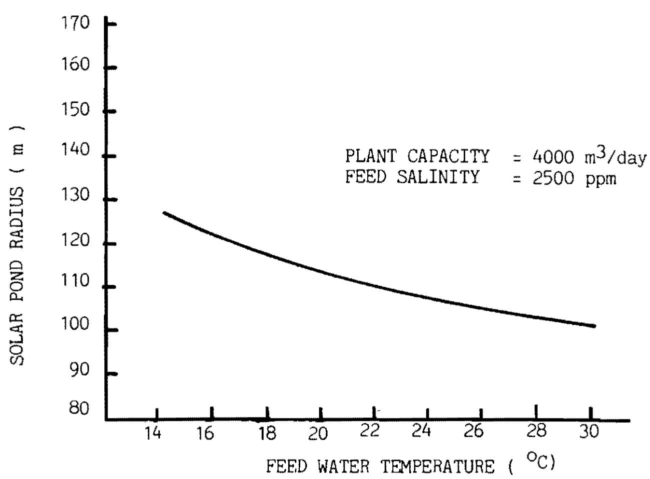


*Figure 7. Effect of Feed Water Temperature on Solar Pond Radius*

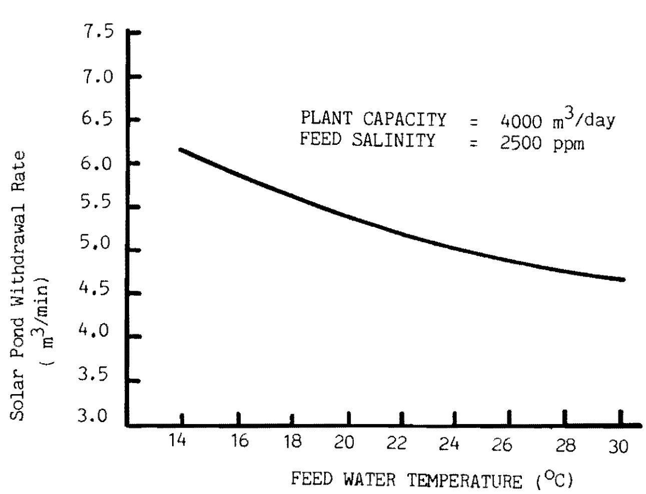


*Figure 8. Effect of Feed Water Temperature on Solar Pond Withdrawal Rate*

The capital cost of the desalination plant is quite sensitive to the feed water temperature since this temperature directly affects the cost of the solar pond and the two heat exchangers. Figure 9 shows how these costs vary for a plant capacity of 4000 $m^3$/day and a feed having a TDS of 2500 ppm. It should be noted that the major capital cost item of the plant is the solar pond which amounts to about 74% of the total cost [8].

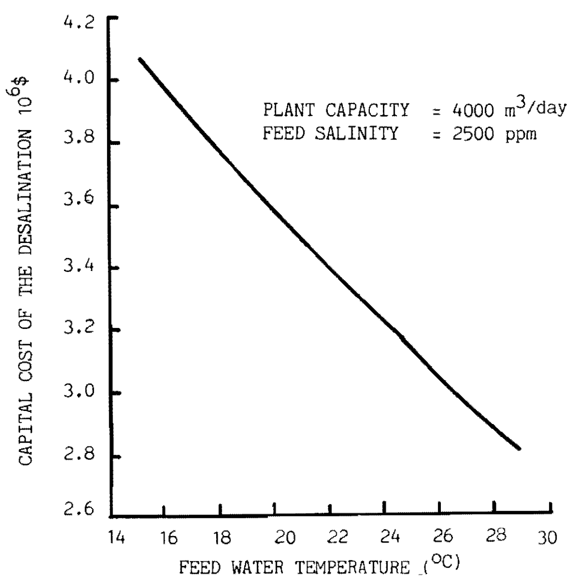


*Figure 9. Effect of Feed Water Temperature on Plant's Capital Cost*

### 6.2. Effect of Feed Water Salinity

Increasing feed water salinity results in a higher main heat exchanger area as shown in parametric form in Figure 10. This is due to a higher regenerant flow rate—and a corresponding higher thermal load— requirement as compared with feed water of low salinity. An increase in the main heat exchanger area of 45% will be obtained as a result of increasing the feed water salinity from 1500 to 2500 ppm TDS for a plant having a capacity of 4000 $m^3$/day.

The solar pond area increases as a result of increasing the feed water salinity—and plant capacity—as shown in Figure 11. This is also a direct consequence of increasing the thermal load on the solar pond. For a plant capacity of 4000 $m^3$/day and a feed salinity of 1500 ppm TDS, the solar pond radius requirement is 100 m. As the feed salinity increases to 2500 ppm TDS the radius increases to 130 m.

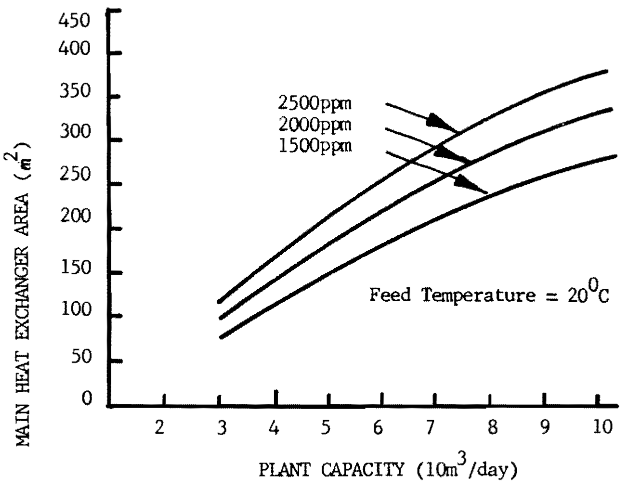


*Figure 10. Effect of Feed Salinity on Main Heat Exchanger Area*

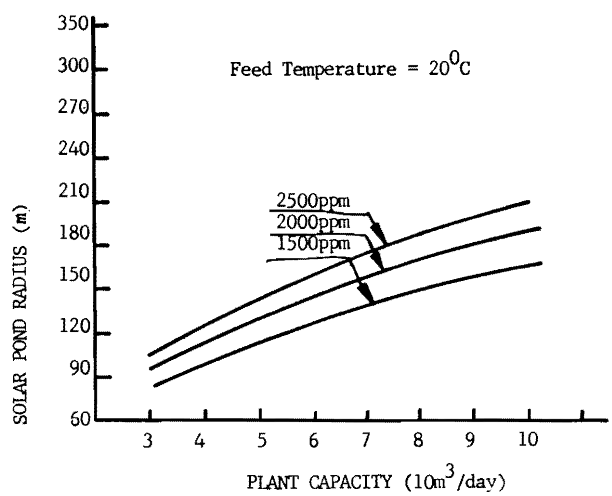


*Figure 11. Effect of Feed Salinity on Solar Pond Radius*

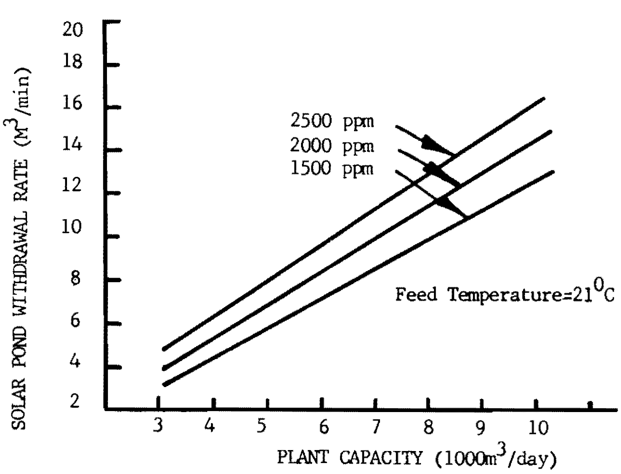


*Figure 12. Effect of Feed Salinity on Solar Pond Withdrawal Rate*

The fluid withdrawal rate from the pond versus plant capacity with feed water salinity as a parameter is shown in Figure 12 with feed water temperature being 21°C. It can be seen that increasing the feed water salinity for a particular plant capacity results in an increase in the withdrawal rate from the pond which is due to a resulting increase in the thermal load on the pond. The withdrawal rate increases by 40% for an increase in salinity from 1500 ppm TDS to 2500 ppm TDS for a plant capacity of 4000 $m^3$/day. The withdrawal rate is also seen to vary linearly with plant capacity.

The effects of feed water salinity on the capital cost of the plant is shown in Figure 13 for three different salinities: 1500, 2000 and 2500 ppm TDS. Both of these cost figures are seen to increase by increasing the feed water salinity as can be expected from the above argument.

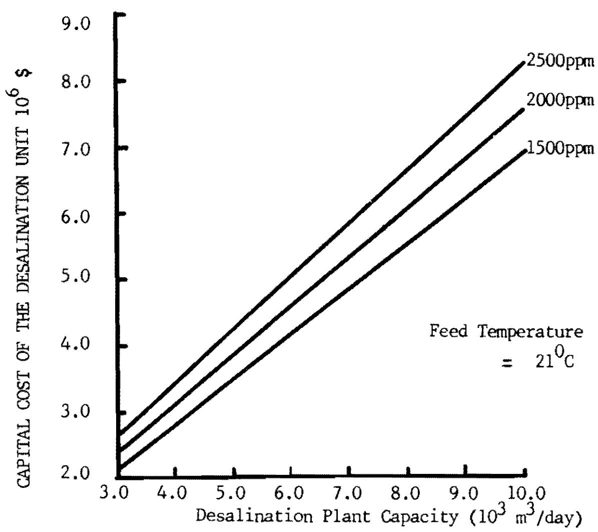


*Figure 13. Effect of Feed Salinity on Desalination Unit's Cost*

### 6.3. The Preheater Effectiveness

The effectiveness of the preheater $\varepsilon$ affects the overall plant design in a profound manner since it is expected to affect the size of the solar pond and the main heat exchanger. It should be pointed out that the effectiveness of the main heat exchanger is uniquely related to that of the preheater since the outlet feed water temperature from the main heat exchanger should always be 80°C (based on the optimization study of the IX resin).

The effect of $\varepsilon$ on the heat transfer areas of the preheater and main heat exchanger are shown in Figure 14 for a plant capacity of 4000 $m^3$/day and feed salinity of 2500 ppm TDS. The area of the preheater is seen to increase almost exponentially with increase the effectiveness of the preheater. The main heat exchanger area, on the other hand, decrease gradually as $\varepsilon$ increases. The dramatic increase in preheater area is the combined result of increasing the thermal load and reduction in the average temperature difference for heat transfer. The reduction in the main heat exchanger area is mainly the result of a lower thermal load.

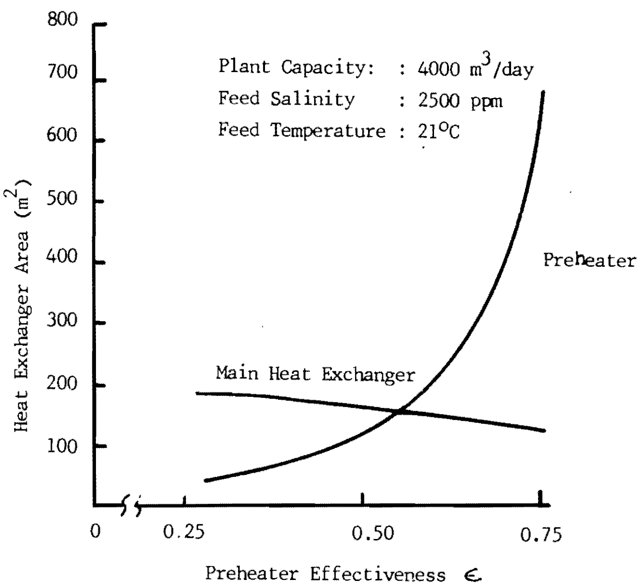


*Figure 14. Preheater Effectiveness Versus Heat Exchanger Area*

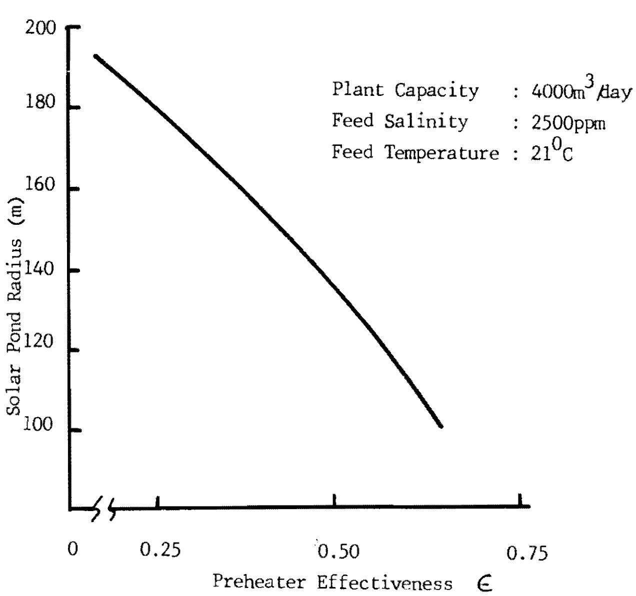


*Figure 15. Preheater Effectiveness Versus Solar Pond Radius*

Figure 15 shows the effect of $\varepsilon$ on the solar pond radius and indicates the potential of a substantial reduction in solar pond area [and cost] when operating at high value of $\varepsilon$. This is particularly important since, as mentioned before, the solar pond represents the largest capital cost component for the plant.

The capital cost of the desalination plant is very sensitive to the value of the effectiveness as can be seen from Figure 16.

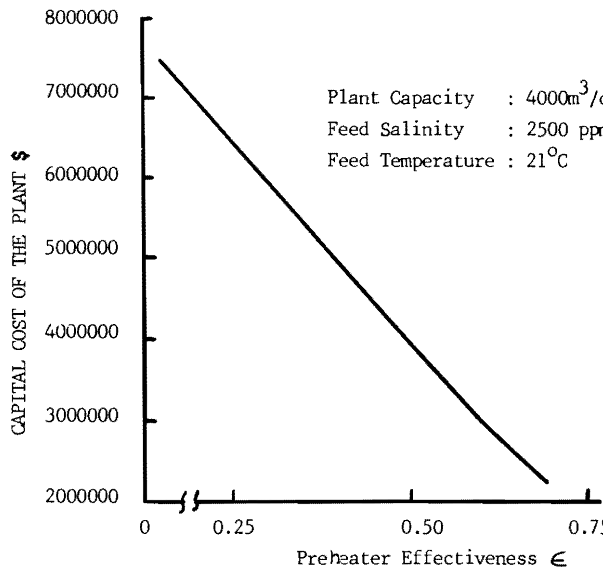


*Figure 16. Preheater Effectiveness Versus Capital Cost*

## REFERENCES


[1] C. D. King, *Separation Processes*. New York: McGraw-Hill, 1971.

[2] F. Helfferich, *Ion-Exchanger*. New York: McGraw-Hill, 1962.

[3] K. Donfner, *Ion-Exchangers*, Ann Arbor Science Publishers, Inc., 1972.

[4] N. H. Nie, C. H. Hull, J. G. Jenkins, and D. H. Bent, *Statistical Package for the Social Sciences*. McGraw-Hill, 1975.

[5] A. A. Afifi and S. P. Azen, *Statistical Analysis, a Computer Oriented Approach*. New York: Jovanovich Publishers, 1979.

[6] M. Edesses, J. Henderson, and T. S. Jayadev, *Simple Design Tool for Sizing Solar Ponds*. SERI/RR-347, Dec. 1979.

[7] W. C. Dickinson and P. N. Cheremisinoff, *Solar Energy Technology Handbook*. Part A, Marcel Dekker, Inc., 1980.

[8] A. A. Kerestecioğlu, 'Solar Desalination with Thermally Regenerable Ion-Exchange Resins', *M.Sc. Thesis*, Florida Institute of Technology, 1981.

[9] W. M. Kays and A. L. London, *Compact Heat Exchangers*. New York: McGraw-Hill, 1964.

[10] A. P. Fargas and M. N. Ozisik, *Heat Exchanger Design*. New York: Wiley, 1965.

[11] R. H. Perry and C. H. Chilton, *Chemical Engineer's Handbook*. Fifth Edition, New York: McGraw-Hill, 1973.

[12] T. T. Shih and R. L. Pigford, 'Removal of Salt from Water by Thermal Cycling of Ion-Exchange Resins', in *Recent Developments in Separation Sciences*, Vol. III, $NNL_i$ (Edition), CRC Press, 1977.

[13] H. Tabor, 'Solar Ponds Larger Area Collectors for Power Production', *Solar Energy*, **7** (1963), pp. 189–194.

[14] H. Weinberger, 'The Physics of Solar Pond', *Solar Energy*, **8** (1964), p. 45.

**Paper Received 28 March 1982; Revised 2 February 1983.**